Flooding, Holdup, and Drop Size Measurements in a Multistage Column Extractor

The hydrodynamics of a pilot plant multistage mixer column extractor was studied for the toluene/water physically equilibrated system. The effects of rotational speed, and continuous and dispersed phase flow rates were investigated under a variety of operating conditions. Dispersed phase axial holdup profiles, determined by a noninvasive ultrasonic method, showed a strong nonuniformity. Depending on the operating conditions, holdup profiles can change from a concave shape to a sigmoidal form with a maximum in the bottom of the column. Sauter mean diameter and drop size distribution profiles are strongly affected by rotational speed. Significant, but weaker, are the effects of continuous and dispersed phase flow rates. Continuous monitoring of the holdup profile in the proximity of flooding leads to the formulation of proper criteria for the prediction of flooding. These criteria are appropriate for models allowing for axial variation of the holdup along the contactor.

V. I. Kirou, L. L. Tavlarides, J. C. Bonnet, C. Tsouris
Department of Chemical Engineering and Materials Science
Syracuse University
Syracuse, NY 13244

Introduction

Solvent extraction has long been a key operation in many processes for product purification and raw material recovery. Two-phase liquid-liquid countercurrent column extractors have been widely used and have been extensively investigated. In early efforts, operation was characterized in terms of the height of the transfer unit and flooding characteristics (Scheibel, 1948; Logsdail et al., 1957; Oldshue and Rushton, 1962). This global approach is still used. The recently published *Handbook of Solvent Extraction* (Lo et al., 1983) provides a guide to the selection and design of such equipment. The design techniques outlined demonstrate that an experimental-empirical approach is employed in the absence of a fundamental unifying theory.

It is recognized that liquid flow patterns inside the contactors have a significant bearing on the column output. Specifically, large deviations from countercurrent plug flow, commonly known as backmixing, lower the concentration driving force and reduce the column efficiency. Backmixing models have been developed for use in extractor design (Sleicher, 1959; Miyauchi and Vermeulen, 1963). The models developed so far simply extend the backmixing models for a single phase and do not consider the special implications of the distributed nature of the dispersed phase. For example, continual drop coalescence and redispersion result in the drop size distribution, which in turn causes a spread in the drop velocity and mass transfer rates.

It has been demonstrated (Olney, 1964) that for a mechanically agitated extractor creating a wide drop size distribution, monodispersed models do not describe with sufficient accuracy the mixing of the dispersed phase and the solute mass transfer.

Only recently has the dispersed phase been treated realistically. Cruz-Pinto and Korchinsky (1980, 1981) considered the effect of drop breakage in a countercurrent rotating disc contactor (RDC). Jiricny and coworkers (1979a, 1979b, 1980) proposed a cell-in-series model to predict dispersed phase axial holdup profiles in a Karr vibrating column. Sovova (1983) developed a simulation model of the dispersed phase holdup in a vibrating plate extractor. Drop population balance equations were proposed to model the various stages of the column, and the equations accounted for the droplet rate processes of coalescence, breakup, and interstage transport. Predicted holdup profiles and drop size distributions were found to be in good agreement with experimental data. Steiner et al. (1984) predicted drop size distributions, axial holdup profiles, and flooding performance in a Kuhni column. The adoption of a drop size distri-

Correspondence concerning this paper should be addressed to L. L. Tavlarides. J. C. Bonnet is with Escuela de Ingenieria Quimica, Universidad Central de Venezuela, Caracas, Venezuela.

bution based on a simple geometrical class division substantially reduced the amount of computation.

It can be concluded that the modeling of the column hydrodynamics without mass transfer is well advanced. However, a comprehensive column model has not yet been formulated, which takes into account quantitatively the phenomena:

1. Dispersed phase droplet processes (breakage and coalescence)
2. Microscopic interphase transport processes
3. Macroscopic flow patterns in the extractor

has not yet been formulated.

Previous work in this group (Coulaloglou and Tavlarides, 1977; Hsia and Tavlarides, 1980; Bapat et al., 1983) has accumulated considerable information on the functioning of a continuous-flow stirred-tank reactor (CFSTR). Logical extension of this work is the investigation of the performance of a multistage mixer column. The Oldshue-Rushton column (ORC) has been chosen, since, by representing a vertical sequence of CFSTR's it renders simpler the extensions-modifications of the existing algorithms and provides a direct test of the underlying models.

Experimental work in ORC's is limited. Recent hydrodynamic studies of flooding and/or phase inversion, holdup, and drop size distribution are summarized below. Flooding in ORC's is characterized by the complete rejection of the dispersed phase through the aqueous phase inlet line (Sarkar et al., 1985). Phase inversion, a close loading point but a different phenomenon (Luhnining and Sawistowski, 1971; Sarkar et al., 1980), has also been observed in ORC's. It seems that there is disagreement among investigators whether flooding or phase inversion or both are observed in ORC's. Arnold et al. (1974), studying the toluene/water physically equilibrated system observed flooding outside the impeller Reynolds number range 1.075×10^4 to 2.15×10^4, with phase inversion occurring inside this range. Sarkar et al. (1985) studied the same system but recorded only flooding over a wide range of operating conditions. Komasawa and Ingham (1978) observed phase inversion at an impeller Reynolds number $Re_I = 0.73 \times 10^4$ (solute-free case). Sarkar et al. (1980) studied the limiting capacity of rotary agitated columns and recorded only phase inversion for the butyl acetate/water system. For the same system, Sarkar et al. (1985) recorded phase inversion occurring in an "erratic manner" with "no consistent behavior." Further study was suggested to determine the proper criteria for the limiting capacity of rotating contactors in general and ORC's in particular.

Similarly, disagreement seems to exist regarding holdup and drop size data. Komasawa and Ingham (1978) reported an $N^{2.5}$ dependence of overall holdup values, whereas Sarkar et al. (1985) correlated holdup data according to N^1. The former indicated a strong continuous and dispersed phase flow rate dependence; the latter indicated a strong dispersed phase flow rate dependence but did not investigate (or mention) the continuous phase flow rate dependence. The change of Sauter mean diameter was found to be insignificant along the column height by Komasawa and Ingham, whereas a twofold decrease was shown by Arnold et al. (1974), for certain operating conditions. A similar decrease was reported by Sarkar et al. (1985), but 10–40% larger mean drop sizes were found when data were compared with a correlation due to Arnold et al. (1974).

The main reasons for the disagreements are the lack of reliable correlations with which data from various investigations can be compared, the complexity of the involved experimental measurements, the limitations of the methods of measurement (Sarkar et al., 1985), and the complete absence of a unifying theory to predict the hydrodynamic behavior of such contactors under various operating conditions.

In this work a fully instrumented seven-stage ORC has been commissioned in order to provide reliable data to corroborate and improve computer models to predict column performance. The main features of the column include five sampling probes for measurement of axial profiles of drop size distributions and six stations for dispersed phase holdup profile measurement by a novel ultrasonic method (Bonnet and Tavlarides, 1987). Uncontaminated-phase sampling probes for mass transfer data and backmixing studies have also been developed to be used in future work.

In this work the hydrodynamics of the column is studied for the physically equilibrated toluene/water system. The flooding behavior of the contactor is investigated, and axial profiles of holdup and drop size distribution are measured under a variety of experimental conditions. The results are compared with previous invetigations.

Experimental Method

Figure 1 is a diagram of the experimental setup, including the contactor and the employed instrumentation. A multistage mixer column of the Oldshue-Rushton type (ORC) is used in this work. The column main section consists of a 12.7 cm dia., 110 cm long glass pipe divided into seven compartments each 12 cm high. The diameter of the six-blade impellers, located centrally in each stage, is 6.35 cm and that of the stator openings 6.86 cm, allowing a 29% free area. Teflon annular gaskets are sandwiched between two identical type 316 stainless steel pieces which form each stator, to eliminate any clearance between the plates and the column wall. There are twelve 2.5 cm dia. ports drilled into the column walls to permit insertion of microphotographic probes, thermocouples, tracer-injection lines, and probes for sampling uncontaminated phases (the latter are used for backmixing and mass transfer experiments). In addition there are seven pairs of 3 cm dia. flat polished slots for mounting ultrasonic transducers used in holdup measurements. Organic phase feed is introduced through a distributor. The distributor consists of 48 type 316 stainless steel nozzles of 0.15 cm ID welded on a stainless steel plate. The plate is mounted on a Teflon parallelepiped base that consists of three sections connected together. The middle section is a solid Teflon piece that provides support for the shaft. The end sections are hollow parallelepipeds, each connected with half of the nozzles. Based on the correlations due to Scheele and Meister (1968), a critical drop diameter of 0.4–0.5 cm is estimated at a total volumetric flow rate of 650 cm^3/min before jetting occurs. Connected to the main section are the 15 cm dia. bottom and top disengagement sections. Transition from the 12.7 cm main section to the 15 cm disengagement sections is accomplished by conical reducers welded to the main section.

Drop size distribution axial profiles are measured by employing a microphotographic technique that is a modified version of a technique developed by Bapat (1982); it employs the microphotographic probe shown in Figure 2. The basic elements of the probe are a microscope, a camera, and fiber optics. A microflash unit (EG&G #549-11) synchronized with the camera is used as

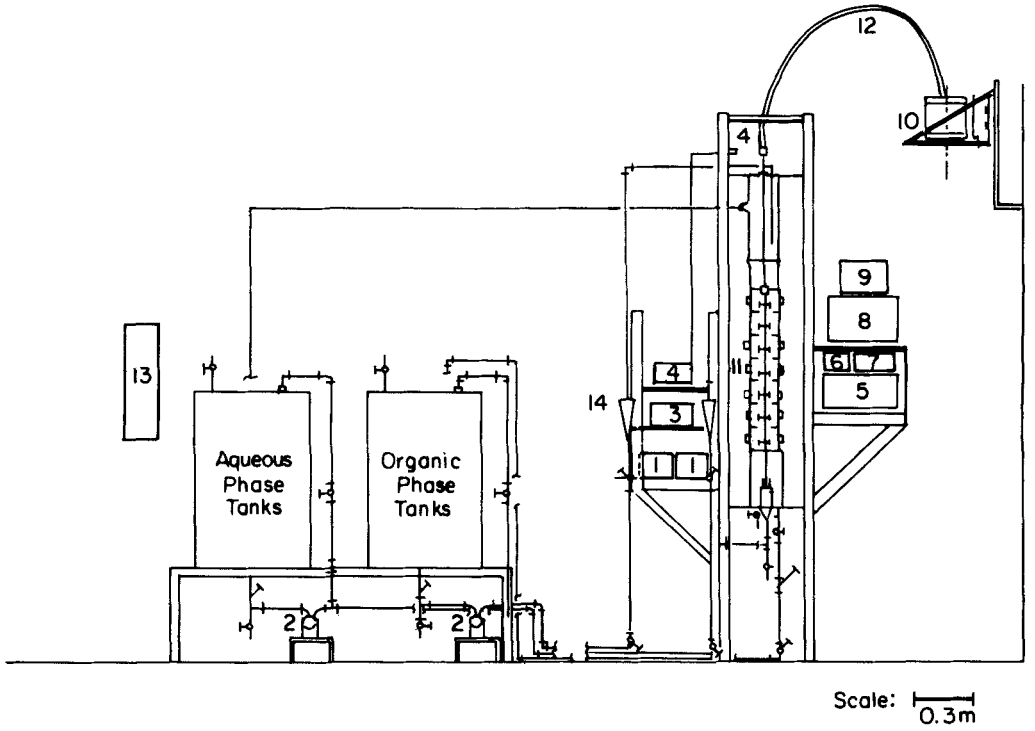

Figure 1. Pilot plant instrumentation.

1. Control box for pumps
2. Peristaltic pumps
3. Digital thermometer (10 thermocouples)
4. Touchless tachometer
5. Oscilloscope (4 channels)
6. Amplifier
7. Pulse generator
8. Microflash
9. Microflash drive unit
10. ½ HP motor, AC
11. Ultrasonic transducers (6 pairs)
12. Flexible shaft
13. Deionizer
14. Flowmeter

a light pulse source. The extremely short duration of the pulses (0.5 μs) essentially freezes the droplet motion and in this way a picture of usually 10–15 drops is taken through the variable-magnification (5–40X) microscope. A rigid image conduit and a flexible trifurcated light guide, used for remote light transmission, complete the assembly. There are totally five microphotographic probes located in the first, third, fourth, fifth, and seventh compartments. Two Kodak Technical Pan Films 2415 were exposed in, usually, the first, fourth, and seven stages, and 500–800 drops per stage were measured by a semiautomatic particle analyzer (MOP-30, Carl Zeiss Inc.) interfaced with an IBM PC computer.

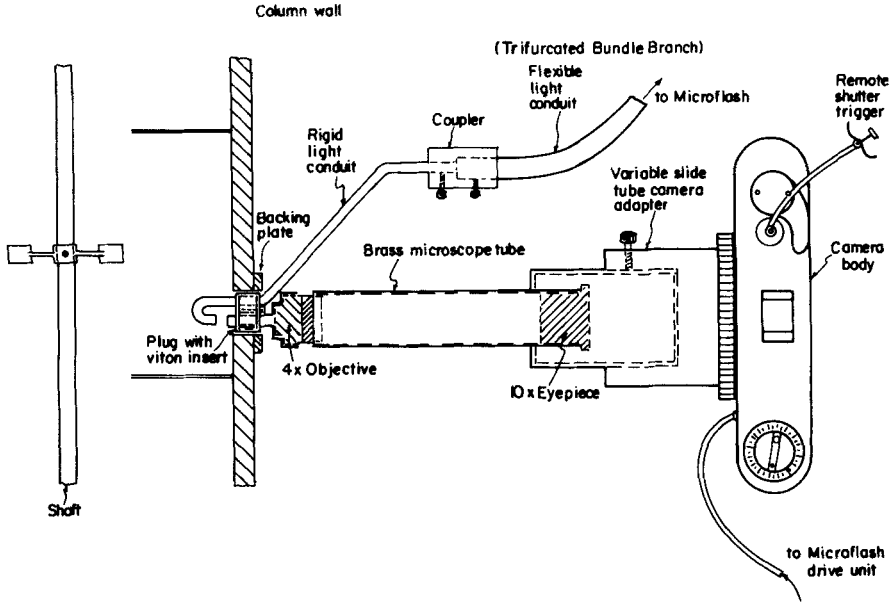

Figure 2. Microphotographic probe.

Holdup measurements using an ultrasonic technique was recently reported by Havlicek and Sovova (1984). In this work an ultrasonic technique developed by Bonnet and Tavlarides (1987) was used for holdup measurements. The technique is capable of measuring the column axial holdup profile in a noninvasive manner under steady state or transient conditions and works as follows. A pulse generator sends a continuous train of electric pulses to a transducer, mounted flush to the flat polished slots discussed above, which in turn emits an ultrasonic pulse through the two-phase medium. An identical transducer positioned on the diametrically opposite side of the column receives the signal and sends it through an amplifier to an oscilloscope that is simultaneously triggered by the pulse generator. The transmittance time necessary for the pulse to travel through the two-phase medium can be calculated from the displayed waveform. Finally, holdup, ϕ, is found by using the relation

$$\phi = \frac{t^* - t_1}{t_2 - t_1} \tag{1}$$

where t_1 and t_2 are the transmittance times of the pure aqueous and the pure organic phases, respectively, and t^* is the transmittance time for the dispersion. A justification for the use of a linear relationship for holdup calculations, Eq. 1, is given in Bonnet and Tavlarides (1987), where a more detailed description of the technique is presented.

Experimental design and procedure

Taking into consideration the independent variables involved and the equipment restrictions, the following ranges of parameters were investigated (nominal values):

Rotation speed: 160–250 rpm (2.67–4.17 rps)

Continuous phase flow rate: 0.3–1.7 L/min (corresponding superficial velocities, 0.039–0.234 cm/s)

Dispersed phase flow rate: 0.1–0.95 L/min (corresponding superficial velocities, 0.013–0.125 cm/s)

Temperature of experiments: 20°C

The physically equilibrated toluene/water system was used in this work, with toluene being the dispersed phase and water the continuous. The physical properties of the system are summarized in Table 1.

Mutual saturation of the two phases preceded the actual runs. When the saturation step was finished, samples of the two phases were taken and the physical properties of the system were measured. A wire torsion tensiometer (Fisher Surface Tensiomat, model 21) was used to measure interfacial tension. The viscosities of the liquids were measured by a Cannon-Fenske viscometer. Toluene content of the aqueous phase was measured by using a UV-visible spectrophotometer (Perkin Elmer Model 559).

Table 1. Physical Properties of the System Studied

Density of continuous phase	1.00 g/cm^3
Density of dispersed phase	0.86 g/cm^3
Viscosity of continuous phase	1.0 cp [mPa · s]
Viscosity of dispersed phase	0.6 cp [mPa · s]
Interfacial tension	31.9 dyn/cm

During a typical run the column was operated for 30–45 min before steady state was reached. During this time the holdup was measured four to five times and only when the holdup profile had not changed for at least 10 min was the steady state assessed. Then photographs were taken as described in the previous section.

During flooding experiments the holdup profile was recorded and the dispersed phase flow rate was increased after the assessment of the steady state in the column. The column was then operated under the new conditions for adequate time until a new steady state or flooding was reached. More details about the experimental setup and the execution of the experiments are given elsewhere (Kirou, 1987).

Results and Discussion

Flooding

Flooding is characterized by the rejection of a fraction of the dispersed phase as a dense layer of drops. This behavior is similar to the flooding observed by Sarkal et al. (1985). Flooding in this study is easily recognizable and the reproducibility of flooding rates is within ±5%. The flooding behavior is similar under all conditions and can be described as follows. As the system conditions are approaching flooding the lower stages of the column show large holdup values (~45–50%). Droplets, in a close-packing form, are continuously touching each other but coalescence is moderate, so that large masses of uncoalesced drops are periodically moving back and forth without being able to escape to the upper stages. This description of the hydrodynamics is representative of the region close to the wall and beneath the stators of the lower stages. In the impeller region droplet movement and coalescence are more intense and the whole picture resembles an inactive shell about 1–2 cm thick, with an active nucleus located around the impeller. More activity can also be observed in the upper stages, especially the sixth and the seventh, where the holdup is obviously lower.

Emulsion-type flooding was observed under all investigated conditions (in terms of impeller Reynolds number, $1.075 \times 10^4 < Re_I < 1.680 \times 10^4$). Phase inversion was not observed under the selected operating conditions, contrary to the observations of Arnold et al. (1974) and Komasawa and Ingham (1978).

The results of a typical flooding experiment are shown in Figure 3. The change of the holdup profile as dispersed phase flow

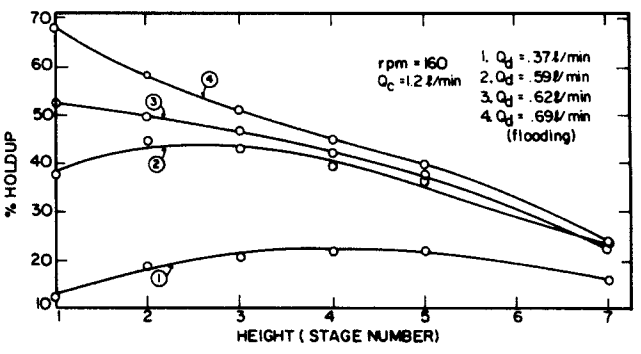

Figure 3. Results of a typical flooding experiment.

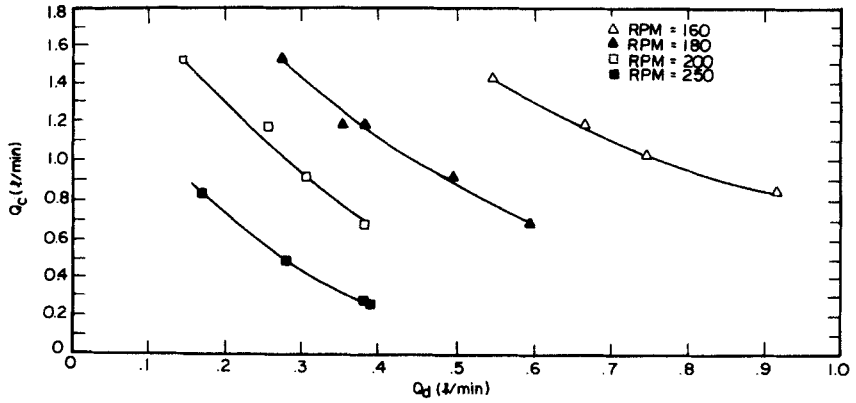

Figure 4. Continuous vs. dispersed phase flow rates at flooding with rpm as a parameter.

rate increases, follows a certain pattern that was reproducible throughout the course of this work, under a variety of experimental conditions. Far from flooding conditions, the holdup profile yields a maximum in the upper stages of the column. As dispersed phase flow rate increases, the maximum shifts to the middle and then to the lower stages of the column. At flooding the holdup profile has a sigmoidal shape with a maximum in the first stage. The average holdup in the column is betwen 30 and 40%, with a value of 50–70% in the first stage. The value of holdup in the top of the column (seventh stage) is three to four times smaller than the value of holdup in the bottom of the column.

Figure 4 is a performance chart, indicating flooding rates at four different agitation levels. A consistent comparison among the data of various investigators is not possible, since the effect of column configuration (e.g., impeller to column diameter ratio, stage height to column diameter ratio, stator free area, etc.) is not completely understood, and no flooding correlations are available for ORC's. Nevertheless, flooding rates in the present study are three to six times lower than the flooding rates reported by Arnold et al. (1974) and Sarkar et al. (1985). A reason for this dramatic difference in capacity probably comes from the difference in the impeller to column diameter ratio, which is 1/2 in the present study whereas the other two references report a 1/3 ratio. This geometric difference produces different hydrodynamic characteristics of the flow field even if the power input per unit volume is the same. For example, at a power input per unit volume of the order of 100 W/m^3, the pumping capacity and the impeller Reynolds number in this contactor are three and two times larger, respectively, than these quantities in the column used by Sarkar et al. (1985).

Besides these differences in the macroscopic hydrodynamic characteristics of the contactors, an important piece of information in comparing or explaining the flooding behavior of various contactors is the existence of subcritical drops inside the column (subcritical drops are those that move cocurrently with the continuous phase). These drops are formed all over the contactor but are entrained in the lower section of the column due to their small rising velocity. Jiricny et al. (1979b) showed that the accumulation of these tiny drops in the bottom of column can change drastically the shape of holdup profiles and can eventually lead to flooding. Similarly, Steiner et al. (1984) attributed flooding to the accumulation of these tiny drops in the continuous phase disengagement section. Unfortunately, previous studies in ORC's do not report drop size distribution profiles (only Sauter mean diameter profiles are reported) and consequently comparisons among the data of various investigators are difficult. In the present design, accumulation of tiny drops is favored underneath the lower stator of the first stage because of the sudden expansion from the 12.7 cm dia. main column section to the 15.2 cm dia. continuous phase disengagement section. This increase in the cross-sectional area leads to a decrease in the continuous phase superficial velocity in that region and consequent accumulation of tiny drops, which may form a dense layer if the dispersed phase flow rate continues to increase. This layer of drops eventually travels downward to the exit line of the continuous phase and leads to flooding.

In an attempt to quantify exact criteria for the prediction of column flooding—to be used in the modeling part of this project—a small number of flooding experiments was conducted with *a priori* known flooding rates. In these replicate experiments initial continuous and dispersed phase flow rates were very close to the flooding rates and small increments in either of the two flow rates were slowly imposed. Typical results are shown in Figures 5a and 5b, where holdup profiles are indicated in the proximity of flooding, as dispersed or continuous phase flow rates increase. Total time of execution of experiments is also shown. It is interesting to notice that apart from the section of the contactor where flooding appears (first and second stage) the holdup profile changes in the rest of the contactor even at flooding. In figure 5a it is observed that the holdup values of the third up to the seventh stages slightly increase with small increases in the dispersed phase flow rate. These results imply that the dispersed phase feed is not completely rejected with the exiting continuous phase, but a part of it moves to the upper stages. On the other hand, the steady state profiles that develop by increasing the continuous phase flow rate displayed in Figure 5b show a slight decrease in holdup after flooding is reached. This decrease occurs since the increased continuous phase flow rate carries a larger portion of dispersed phase downstream. At any rate, Figures 5a and 5b clearly indicate that the proper criteria for flooding prediction are:

$$\min\left(\frac{\partial \phi_i}{\partial Q_d}\right) = 0, \quad i = 1, 2, \ldots, M$$

and

$$\phi_i > \phi_j, \quad j = 1, 2, \ldots, i-1, i+1, \ldots, M \qquad (3)$$

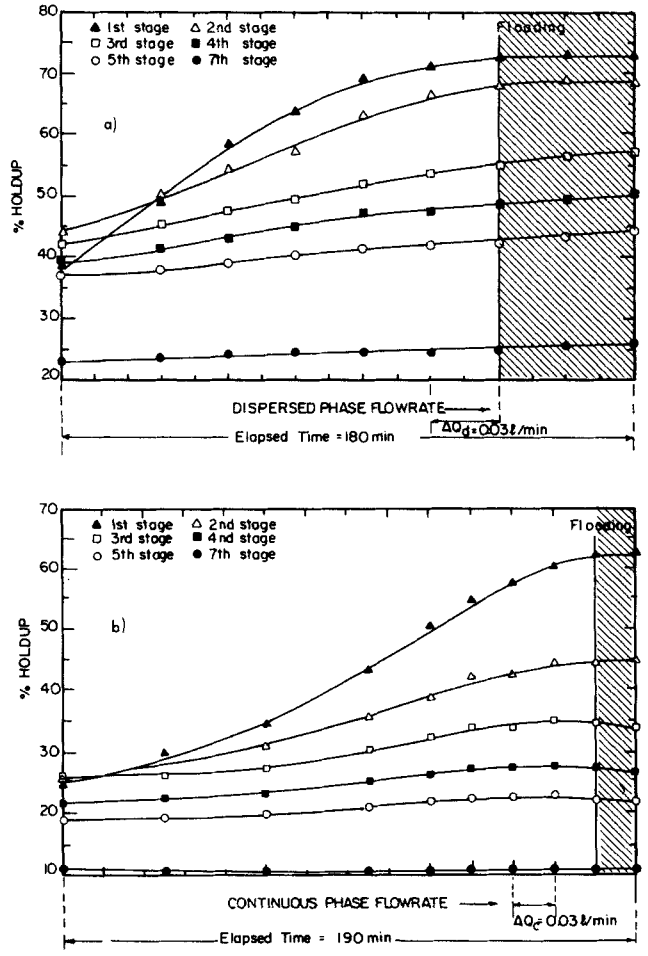

Figure 5. Holdup values along contactor in proximity of flooding: (a) incremental changes imposed on dispersed phase flow rate and (b) incremental changes imposed on continuous phase flow rate.

or,

$$\min\left(\frac{\partial \phi_i}{\partial Q_c}\right) = 0, \quad i = 1, 2, \ldots, M$$

and

$$\phi_i > \phi_j, \quad j = 1, 2, \ldots, i-1, i+1, \ldots, M \qquad (4)$$

where M is the number of stages. The inequality $\phi_i > \phi_j$ simply states that flooding occurs at the stage with the highest holdup. It should be noted here that criteria to predict flooding in columns are well established for models employing the concept of slip velocity and, therefore an average value of holdup. However, proper criteria for models employing variable holdup values along the contactor have not been reported in the literature. The only exception is the modeling work of Jiricny et al. (1979b). However, the validity of the postulated criterion was not tested and no conclusions were drawn regarding its applicability. In summary, a "conventional" type of flooding, characterized by the rejection of dispersed phase as a dense layer of drops has been observed. Flooding is easily recognizable and flooding rates are reproducible within ±5%. Finally, criteria appropriate for models employing variable holdup profiles are suggested and tested with experimental results.

Holdup

The effects of agitation intensity and flow rates on holdup were investigated in this work. The effect of rotor speed is shown in Figure 6a. At low rpm, the holdup presents a weak maximum in the upper stages of the column. As rpm increases, the average holdup increases and the maximum shifts towards the middle of the column. At even higher rpm, the maximum is located in the lower part of the column. A maximum in the first stage (not shown in the figure) will appear if the rpm is further increased. Similar effects are observed with the increase of the continuous and dispersed phase flow rates. Figures 6b and 6c show that, for low flow rates, the holdup profile presents a maximum in the upper or middle sections of the column. As Q_c or Q_d are increased, the maximum shifts to the bottom of the column, and the concave shape of the profile changes to an S-shaped form. No reference was found in the literature mentioning such behavior in an Oldshue-Rushton column, where only monotonically increasing holdup profiles along the column height have been reported (Arnold et al., 1974; Sarkar et al., 1985).

The increase of holdup along the column height was explained (Sarkar et al., 1985) by the gradual decrease in d_{32}, calculated from simultaneously measured drop size distribution profiles. Regarding this explanation, it should be noted that the drop size distribution alone is not always adequate to explain the form of the holdup profiles. Instead, the convective flow of the dispersion, properly incorporated in the population balance equations, should be considered. Obviously, this requires an analysis of the results from a solution of the pertinent equations. Qualitative description is hazardous without careful consideration of the various hydrodynamic phenomena that occur simultaneously. However, it should be clear that the velocity of drops is the vectorial sum of the relative velocity of the drops with respect to the continuous phase and the true velocity of the continuous phase, that is:

$$u_i(d) = v(d, \phi_i) - \frac{V_c}{(1 - \phi_i)} \qquad (5)$$

The first term on the righthand side depends on the drop size distribution and the holdup. If the operating conditions are such that the absolute drop velocity is dominated by drop size as opposed to holdup, then holdup profiles may be explained by the form of the drop size distribution profile alone. However, a maximum in the middle or the bottom of the column may be unexplicable unless the true velocity of the continuous phase—the second term in the above equation—is considered. Notice that this term does not vanish when the continuous phase flow rate is zero, since it includes the backflow in the continuous phase, which depends on agitation and dispersed phase flow rate (Jiricny et al.; 1979a). Moreover, the monotonically increasing form of holdup profiles cannot be justified under all experimental conditions. Instead, a gradual decrease from the bottom to the top of the column should be observed under operating conditions

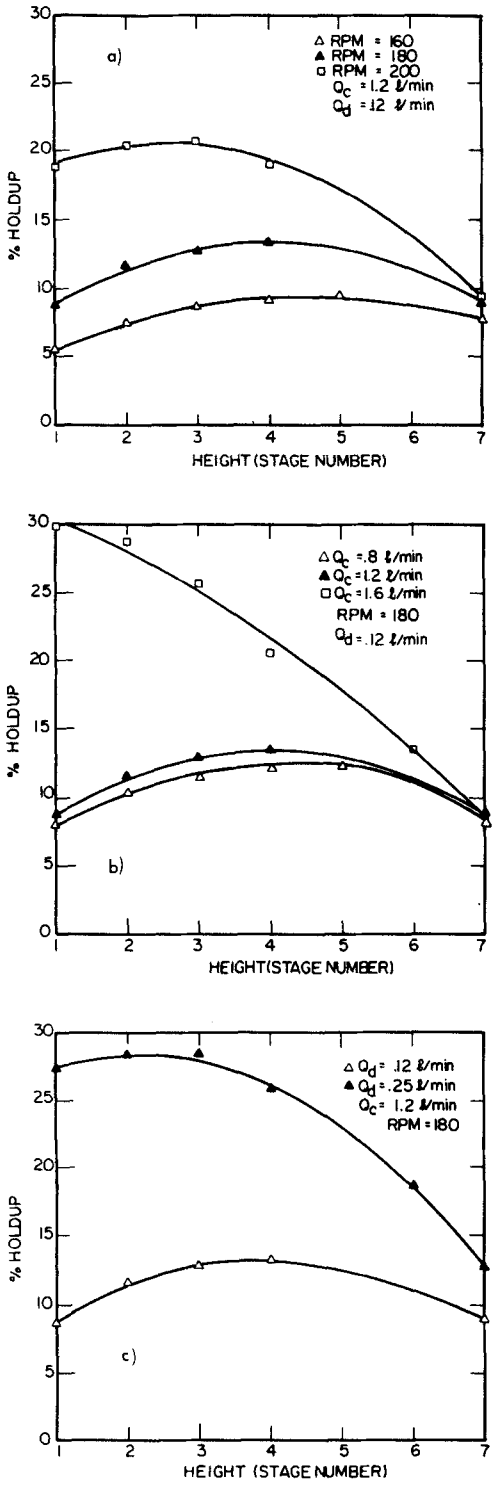

Figure 6. Effect of operating variables on holdup: (a) agitation intensity, (b) continuous phase flow rate, and (c) dispersed phase flow rate.

close to flooding. Flooding is characterized by large holdup values and occurs in that part of the column where holdup is maximum (see the previous section). If the gradual increase form of holdup profile is accepted, then the initiation of flooding will occur in the top of the column. Instead, flooding is most of the times observed to commence in the bottom compartment (Sarkar et al., 1980). In the present study flooding was *always* observed to occur at the bottom of the column (Kirou, 1987). This means that under certain conditions close to flooding, the holdup profile should have a decreasing form. It should be mentioned at this point that concave or sigmoidal profiles have been reported in other types of agitated contactors (Rod, 1971; Jiricny and Prochazka, 1980; Steiner et al., 1984; Sarkar et al., 1985, for the RDC part of the study).

In summary, holdup profiles in the present work show a strong nonuniformity, depending on the operating condition. Rotational speed and flow rates similarly affect overall holdup values and the form of the holdup profile. The latter can change from a concave shape to a sigmoidal form as column operation approaches flooding.

Drop size and size distribution

The effect of rpm on average drop size is indicated in Figure 7. In all cases, the Sauter mean diameter decreases as rpm increases, representing the increased droplet breakup. It is interesting to notice that the mean drop size does not change significantly above the middle of the contractor. This indicates that, at a certain height inside the column, the rate of coalescence becomes equally important with droplet breakup, which is predominant in the entrance section of the column because of the large diameter of the droplets leaving the distributor (0.4–0.5 cm). This observation is valid even at the lower rotor speed, 160 rpm, where the mean diameter reaches 80% of the final value within the first three stages.

The effect of agitation on the drop size distribution (DSD) is shown in Figures 8a and 8b. Here the DSD's are compared at the bottom and the top of the column, respectively, for three different levels of agitation, 160, 180, and 200 rpm. (Note that the scales in the two figures are different.) At both locations (bot-

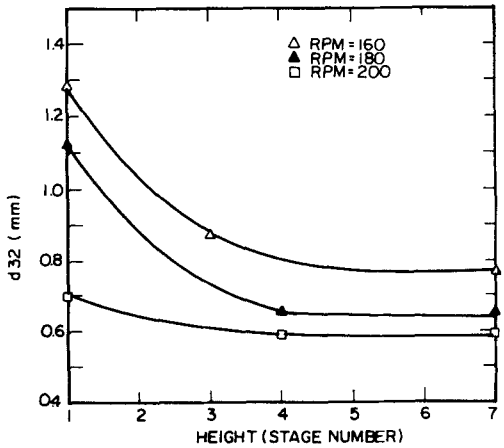

Figure 7. Effect of agitation intensity on mean Sauter diameter.

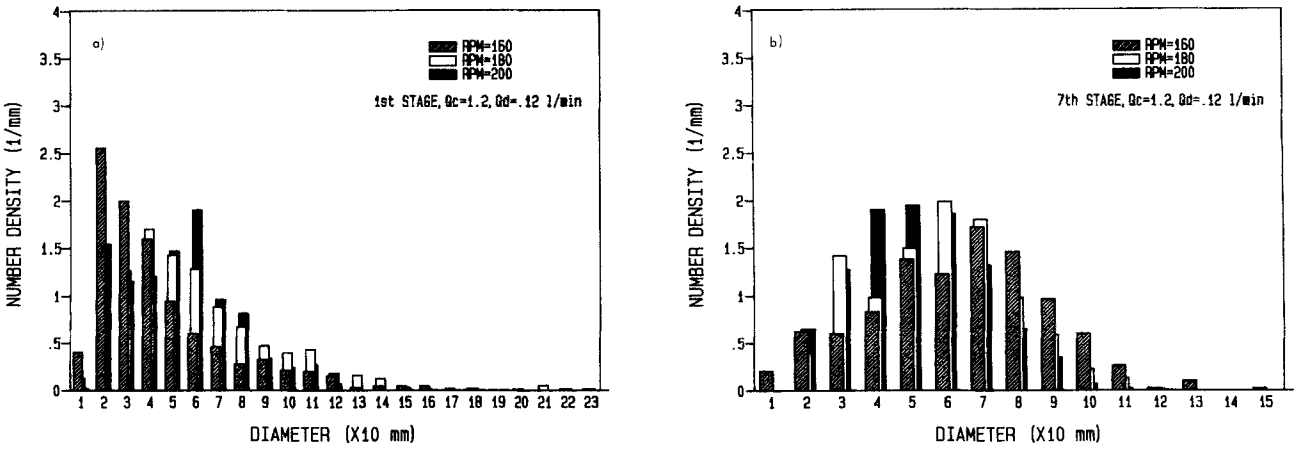

Figure 8. Effect of agitation intensity on drop size distribution: (a) bottom of column, and (b) top of column.

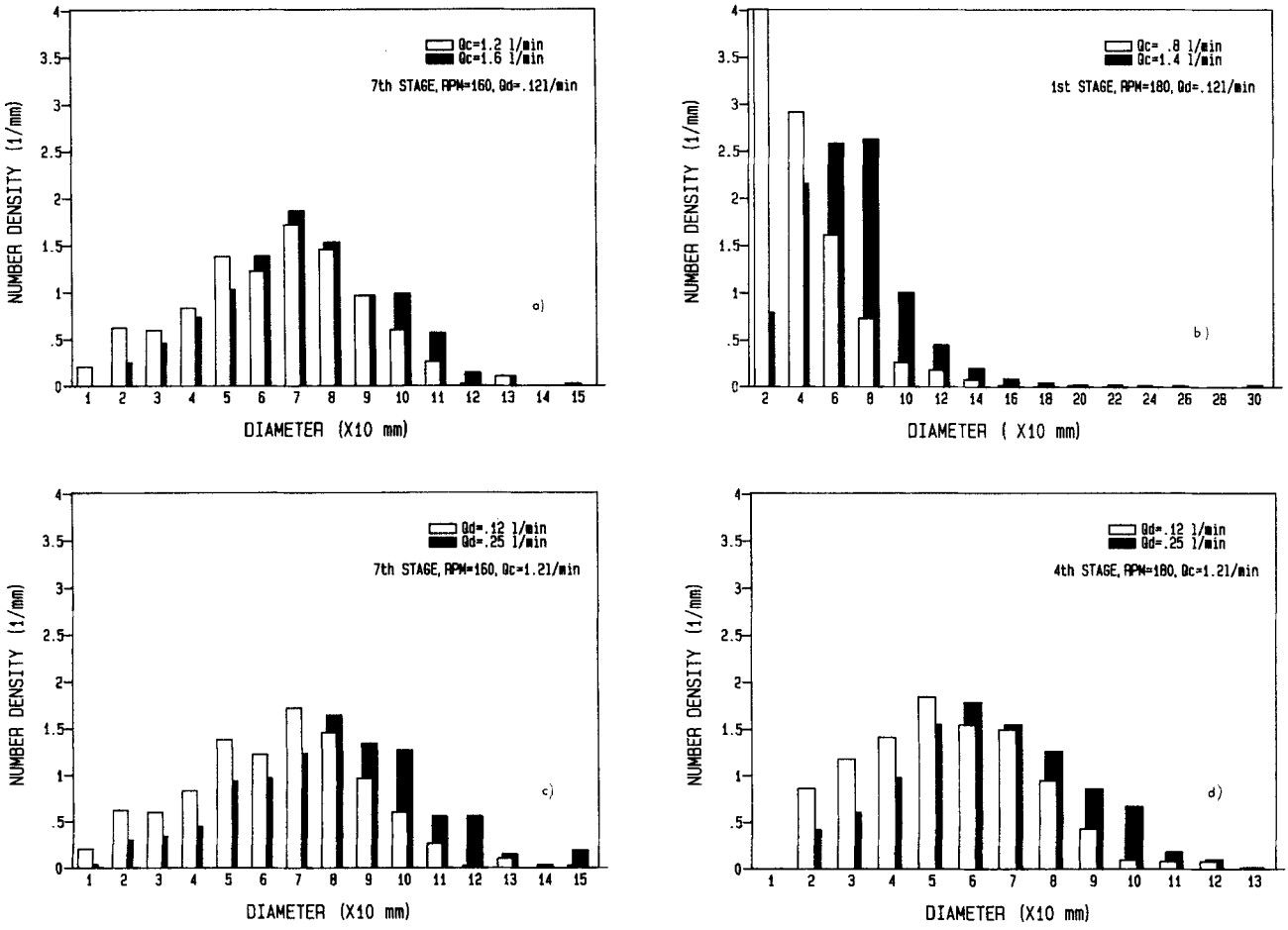

Figure 9. Effect of flow rates on drop size distribution: (a) continuous phase flow rate, top of column, (b) continuous phase flow rate, bottom of column, (c) dispersed phase flow rate, top of column, and (d) dispersed phase flow rate, middle of column.

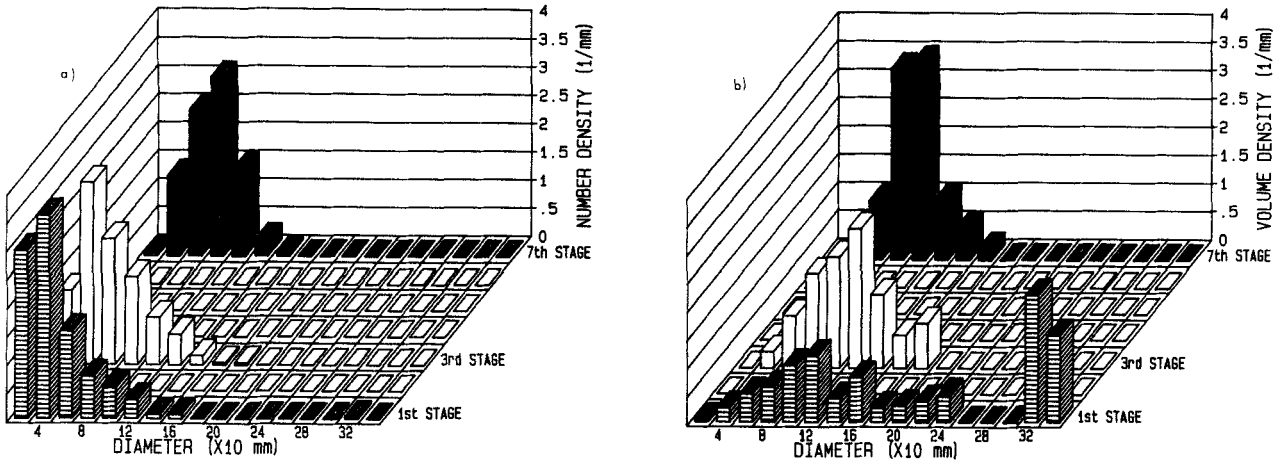

Figure 10. Effect of large drops on volume density function: (a) number density function and (b) volume density function. Operating conditions: rpm = 160; Q_c = 1.2 L/min; Q_d = 0.12 L/min.

tom and top) higher rpm leads to a narrower and more symmetric distribution around the mean value. This trend is reflected in a 20–30% decrease in the standard deviation of the samples of the drop population, as rotor speed increases from 160 to 200 rpm.

Another important point of these figures is the fraction of the tiny drops (<100 μm) in the column. As shown in the figures, as rpm increases from 160 to 200 rpm these tiny drops disappear from both the first and the seventh stages. This result is in accordance with the observation that the number of tiny drops underneath the first stator increases as operating conditions (because of an increase in rpm or flow rates) approach flooding. Figure 9a shows the DSD at the seventh stage for two different continuous flow rates. The data indicate that as Q_c increases from 1.2 to 1.6 L/min the distribution shifts to larger droplet sizes. Similarly, in Figure 9b the DSD at the first stage shifts to larger drops as Q_c increases from 0.8 to 1.4 L/min. Contrary to the observations of Sarkar et al. (1985), the Sauter mean diameter increases up to 10% for a 100% increase in the continuous phase flow rate, over the investigated range. This increase in the droplet size may be attributed to an increase in the entrainment of smaller drops and/or to the higher coalescence rates accompanying the increase in the holdup, which is observed at large Q_c conditions.

The effect of dispersed phase flow rate, Q_d, is similar to the effect of Q_c. Figure 9c shows the drop size distribution in the seventh stage. As Q_d increases from 0.12 to 0.25 L/min the distribution shifts to larger drops. The same observation holds for the drop size distribution in the fourth stage, as Figure 9d indicates. As with the continuous phase flow rate, the effect of Q_d is weaker than the effect of rotational speed. For a 100% increase in the dispersed phase flow rate, only a 15% increase in d_{32} was found. The increase in the droplet size may be attributed, as in the case of Q_c, to an increase in the coalescence rate due to the larger holdup values that are observed as Q_d increases. The importance of the large drops in the volume density function is indicated in the three-dimensional plots shown in Figures 10a and 10b. Figure 10a, showing the number density function, indicates the existence of only a few large drops. However, the contribution of these drops to the volume density function is major, as Figure 10b shows.

Finally, in Figure 11 the drop sizes are compared with the following correlation proposed by Arnold et al. (1974):

$$d_{32} = 2.44 \left(\frac{H}{H_T}\right)^{-0.06} \left(\frac{V_t^2 D \rho_m}{\sigma}\right)^{-0.63} \left(\frac{V_k}{V_t}\right)^{0.18} \tag{6}$$

The comparison shows experimental d_{32} values to be always smaller than the predicted values. The deviation ranges from 2 to 40% and is probably due to the difference in the geometry of the columns.

Acknowledgment

Financial support by the National Science Foundation, Grant No. CPE 8310223, and partial support by the Exxon Education Foundation is gratefully acknowledged. J. C. Bonnet would like to acknowledge the support of the Escuela de Ingenieria Quimica, Universidad Central de Venezuela for the sabbatical year. The help of P. Clancy during the execution of preliminary experiments and the instructive criticism of H. Schmidt, who read the manuscript, are gratefully acknowledged.

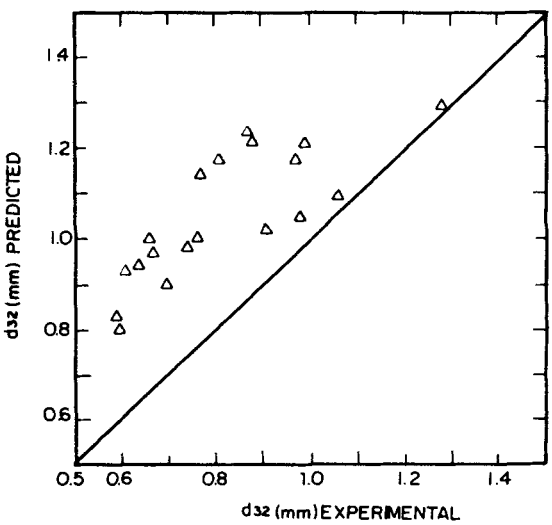

Figure 11. Comparison of experimental results with Eq. 6.

Notation

d = individual drop diameter L
d_{32} = Sauter mean diameter, L
D = impeller diameter, L
H = height, L
H_T = total height of contractor, L
M = number of stages
N = rotational speed, T^{-1}
Q_c = continuous phase flow rate, $L^3 \cdot T^{-1}$
Q_d = dispersed phase flowrate, $L^3 \cdot T^{-1}$
Re_I = impeller Reynolds number
t^*, t_1, t_2 = transmittance times, T
u_i = drop velocity relative to column at stage i, $L \cdot T^{-1}$
v = individual drop velocity in a swarm of drops moving in a quiescent fluid, $L \cdot T^{-1}$
V_c = continuous phase superficial velocity, $L \cdot T^{-1}$
V_d = dispersed phase superficial velocity, $L \cdot T^{-1}$
V_k = characteristic drop velocity, $V_k = \{[(1 - \phi)V_d/\phi]\} + V_c$, $L \cdot T^{-1}$
V_t = impeller blade tip velocity, $V_t = \pi ND$, $L \cdot T^{-1}$

Greek letters

ϕ_i = holdup at stage i
ρ_m = average density of dispersion, $\rho_m = \rho_c(1 - \phi) + \rho_d \cdot \phi$, $M \cdot L^{-3}$
σ = interfacial tension, $M \cdot T^{-2}$

Literature Cited

Arnold, D. R., C. J. Mumford, and G. V. Jeffreys, "Drop Size Distribution and Interfacial Area in Agitated Contractors," *ISEC '74*, **2**, 1619 (1974).

Bapat, P. M., "Mass Transfer in a Liquid-Liquid Continuous-Flow Stirred-Tank Reactor," Ph.D. Thesis, Ill. Inst. Technol., Chicago (1982).

Bapat, P. M., L. L. Tavlarides, and G. W. Smith, "Monte Carlo Simulation of Mass Transfer in Liquid-Liquid Dispersion," *Chem. Eng. Sci.*, **38**, 2003 (1983).

Bonnet, J. C., and L. L. Tavlarides, "An Ultrasonic Technique for Dispersed Phase Holdup Measurements," *Ind. Eng. Chem. Res.*, **36**, 811 (1987).

Coulaloglou, C. A., and L. L. Tavlarides, "Description of Interaction Processes in Agitated Liquid-Liquid Dispersions," *Chem. Eng. Sci.*, **32**, 1289 (1977).

Cruz-Pinto, J. J. C., and W. J. Korchinsky, "Experimental Confirmation of the Influence of Drop Size Distribution on Liquid-Liquid Extraction Column Performance," *Chem. Eng. Sci.*, **35**, 2213 (1980).

———, "Drop Breakage in Countercurrent Flow Liquid-Liquid Extraction Columns," *Chem. Eng. Sci.*, **36**, 687 (1981).

Hsia, M. A., and L. L. Tavlarides, "A Simulation Model for Homogeneous Dispersions in Stirred Tanks," *Chem. Eng. J.*, **20**, 225 (1980).

Jiricny, V., M. Kratky, and J. Prochazka, "Countercurrent Flow of Dispersed and Continuous Phase. I: Discrete Polydispersed Model," *Chem. Eng. Sci.*, **34**, 1141 (1979a).

———, "Countercurrent Flow of Dispersed and Continuous Phase. II: Simulation of Holdup and Particle Size Distribution Profiles," *Chem. Eng. Sci.*, **34**, 1151 (1979b).

Jiricny, V., and J. Prochazka, "Countercurrent Flow of Dispersed and Continuous Phase. III: Measurements of Holdup Profiles and Particle Size Distributions in a Vibrating Plate Contractor," *Chem. Eng. Sci.*, **35**, 2237 (1980).

Kirou, V. I., "Hydrodynamics in a Multistage Column Contactor," M. S. Thesis, Syracuse University (1987).

Komasawa, I., and J. Ingham, "Effect of System Properties on the Performance of Liquid/Liquid Extraction Columns. II," *Chem. Eng. Sci.*, **33**, 479 (1978).

Lo, T. C., M. H. I. Baird, and C. Hanson, eds., *Handbook of Solvent Extraction*, Wiley, New York (1983).

Logsdail, D. H., J. D. Thornton, and H. R. C. Pratt, "Liquid-Liquid Extraction. XII: Flooding Rates and Performance Data for a Rotary Disc Contractor," *Trans. Inst. Chem. Eng.*, **35**, 301 (1957).

Luhning, R. W., and H. Sawistowski, "Phase Inversion in Stirred Liquid/Liquid Systems," *ISEC '71* **II**, 873 (1971).

Miyauchi, T., and T. Vermeulen, "Longitudinal Dispersion in Two-Phase Continuous-Flow Operations," *Ind. Eng. Chem. Fundam.*, **2**, 113, (1963).

Oldshue, J. Y., and J. H. Rushton, "Continuous Extraction in Stirred Liquid/Liquid Systems," *Chem. Eng. Prog.*, **48**, 297 (1952).

Olney, R. B., "Droplet Characteristics in a Countercurrent Contactor," *AIChE J.*, **10**, 827 (1964).

Sarkar, S., C. R. Phillips, C. J. Mumford, and G. V. Jeffreys, "Mechanisms of Phase Inversion in Rotary Agitated Columns," *Trans. Inst. Chem. Eng.*, **58**, 43 (1980).

Sarkar, S., C. R. Phillips, and C. J. Mumford, "Characterization of Hydrodynamic Parameters in Rotating Disc and Oldshue-Rushton Columns. Hydrodynamic Modeling, Drop Size, Holdup, and Flooding," *Can. J. Chem. Eng.*, **63**, 701 (1985).

Scheibel, E. G., "Fractional Liquid Extraction. I," *Chem. Eng. Prog.*, **44**, 681 (1948).

Sleicher, C. A., "Axial Mixing and Extraction Efficiency," *AIChE J.*, **5**, 145 (1959).

Sovova, H., "A Model of Dispersion Hydrodynamics in a Vibrating Plate Extractor," *Chem. Eng. Sci.*, **38**, 1863 (1983).

Steiner, L., M. Laso, and S. Hartland, "Models for Performance of Extraction Columns Based on Actual Drop Behavior," *J. Chem. Eng. Symp. Ser.*, No. 88, 91 (1984).

Manuscript received Mar. 31, 1987 and revision received Aug. 24, 1987.